Hindawi
International Journal of Corrosion
Volume 2018, Article ID 6580750, 11 pages
https://doi.org/10.1155/2018/6580750

Research Article

Corrosion and Leaching Behaviours of Sn-0.7Cu-0.05Ni Lead-Free Solder in 3.5 wt.% NaCl Solution

Jan-Ervin C. Guerrero,[1] Drexel H. Camacho ,[1] Omid Mokhtari,[2] and Hiroshi Nishikawa[2]

[1]*Chemistry Department, De La Salle University, 2401 Taft Avenue, 0922 Manila, Philippines*
[2]*Joining and Welding Research Institute, Osaka University, 11-1 Mihogaoka, Ibaraki, Osaka 567-0047, Japan*

Correspondence should be addressed to Drexel H. Camacho; drexel.camacho@dlsu.edu.ph

Received 6 December 2017; Accepted 5 March 2018; Published 2 May 2018

Academic Editor: Arvind Singh

The corrosion and leaching behaviour of a new ternary Sn-0.7Cu-0.05Ni alloy in 3.5 wt.% NaCl solution is reported herein. Potentiodynamic polarization measurements show that Sn-0.7Cu-0.05Ni has the highest corrosion rate. Results of the 30-day Sn leaching measurement show that Sn-Cu-Ni joint has slight decrease attributed to the formation of thin passivation film after 15 days. The leaching amounts of Sn are observed to be higher in solder joint than in solder alloy due to the galvanic corrosion happening on the surface. EDS and XRD results of the corroded surface confirm that the corroded product is made up of oxides of tin.

1. Introduction

Solder, a fusible metal alloy used to join metal pieces, is a staple material in the electronics industry. It functions as an adhesive or joining material to provide electrical continuity between the active silicon die, the substrate, and the printed wiring boards [1]. Solder alloys made up of tin and lead (Sn-Pb) predominate the manufacturing and electronics industries for years. However, due to the bad effects of lead and its compounds to human health and the environment [2], its use has been widely limited if not banned.

Global lead-free regulations started with the US banning lead (Pb) in gasoline additives, plumbing, and construction [3]. Japan pioneered the use of lead-free solders in the electronics industry and the European Union (EU) passed the restriction of the use of certain hazardous substances (ROHS) in electrical and electronic equipment banning the use of lead, mercury, and cadmium, among others [4]. Thus, there was a critical necessity to look for alternatives to Pb solders for the electronics industry. For solders to be a good environmentally benign substitute to Pb, it should be cost-effective and should mimic the properties of Pb, that is, low melting temperature (around 183°C), good mechanical, thermal, and electrical properties. Almost every lead-free solder in the market is Sn-based solders such as Sn-Ag-Cu and Sn-Cu [1]. At present, there is no common standard for lead-free electronic products since each country or region has its own recommended lead-free solders. In the US, the National Electronic Manufacturing Initiative, Inc., (NEMI) recommends Sn-3.9Ag-0.6Cu as the lead-free solder. Japan, through the Japan Electronic and Information Technology Association (JEITA), recommends the use of Sn-3.0Ag-0.5Cu solder alloy, while the European Consortium recommends Sn-3.8Ag-0.5Cu as the lead-free solder. Overall, the most common type of lead-free solder (LFS) used worldwide is the alloy made up of Sn-Ag-Cu. Alternative Pb-free solder systems such as Sn-Ag, Sn-Bi, Sn-Zn, and Sn-Cu have been developed [1, 5, 6] but uncertainties in their integrity and reliability limited their use in consumer products [7]. New types of lead-free solders are being used by some companies in Japan; Panasonic and Hitachi use Sn-Ag-Bi, Sharp uses Sn-Bi, and Sony uses Sn-Ag-Bi-Cu and Sn-Ag-Bi-Ge solder alloys in their products [3, 4]. New lead-free solder alloys are being studied [8–10] and reliable solders for general and specific applications are still highly sought.

The ternary alloy Sn-0.7Cu-0.05Ni has been shown to be a potential Pb-free solder [11] where the wettability of the alloy was shown to be comparable with some other lead-free

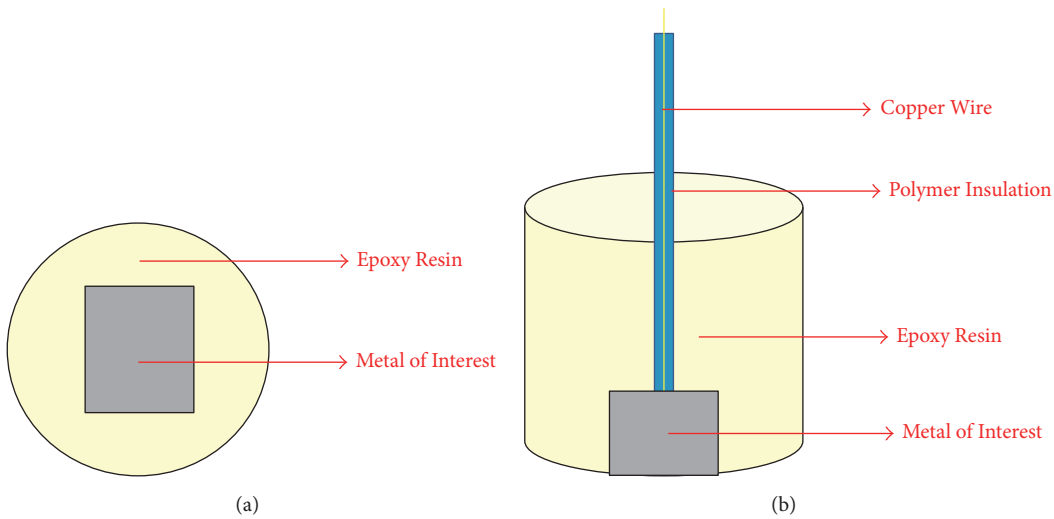

Figure 1: Schematic diagram of the working electrode. (a) Bottom view; (b) side view.

solders [12]. The low experimental wetting angle is a consequence of the addition of Ni in Sn-0.7% wt. Cu. Increasing the amount of Ni also decreases the void percentage and Cu_3Sn growth in Sn-Cu solder alloy [13]. The tensile properties and wettability in solder joints with Cu also improved as a result of adding 0.05 wt.% Ni [14]. The addition of 0.05 wt.% Ni to Sn-0.7Cu solder was shown to effectively reduce the formation of intermetallic compound (IMC) layer at the interface during the reflow process and for inhibiting the growth of IMC during the aging process [15].

To study further the potential of Sn-0.7Cu 0.05Ni solder alloy, there is a need to assess its corrosion behaviour as it is an important factor to consider in formulating new solder materials [16]. The presence of moisture and corrosive salts/ions triggers the corrosion activity of these solder metals affecting the form, fit, and function of the electronic device [17, 18]. Corrosion behaviours of lead-free solders are mainly studied using sodium chloride (NaCl) electrolyte to simulate the seawater condition using different types of lead-free solders [19–24]. Li et al. [20] reported that lead-free solders such as Sn-3.5Ag, Sn-0.7Cu, and Sn-3.8Ag-0.7Cu exhibit better corrosion resistance than Sn-Pb solder in 3.5 wt.% NaCl solution, where Sn-3.5Ag solder was found to be the most resistant among them. Lead-free solder exhibits better corrosion resistant because it exhibits lower passivation current density, lower corrosion current density after the breakdown of the passivation film, and a more stable passivation film on the surface compared to Sn-Pb solder. By investigating the corrosion behaviours of new lead-free solders, the fatigue life of the material can be predicted. A cursory survey of the literature reveals zero investigation on the corrosion behaviour of the new ternary Sn-0.7Cu-0.05Ni alloy. The goal of the present study is to investigate the corrosion resistance of Sn-0.7Cu-0.05Ni as compared to commercially used solder alloys and metal and study the leaching behaviour of tin in the alloys and in their corresponding joints in 3.5 wt% NaCl solution.

2. Materials and Methods

2.1. Materials

2.1.1. Preparation of Working Electrode. The compositions of the solder alloys used in the study are Sn-0.7 wt.% Cu-0.05 wt.% Ni, Sn-3.0 wt.% Ag-0.5 wt.% Cu and Sn-0.8 wt.% Cu, 60 wt.% Sn-40 wt.% Pb, and pure Sn metal. The alloys were cut using low-speed cut-off saw into square blocks (approximate dimension of 0.5 × 0.5 × 0.5 cm). Each metal piece was attached to an insulated Cu wire by hand soldering using the same metal alloy to provide electrical connections and then cold-mounted using epoxy resin as shown in Figure 1. The specimens were ground using SiC paper/sand paper up to 1200 grit, rinsed with distilled water, and cleaned in an ultrasonic cleaner for 2 mins. The surface area exposed to the test solution was $0.5 \pm 0.2\,cm^2$.

2.1.2. Preparation of Solder Alloy and Solder Joint for Leaching Measurement. Solder joints were prepared by joining a previously acid-cleaned (HNO_3/MeOH) copper plate (5 × 10 × 2 mm) with similarly sized lead-free solder plate using a solder paste. The coupled metals were heated on a hot plate at 230°C until the solders stuck on the Cu plate. For leaching experiments, the samples were prepared as shown in Figure 2.

2.1.3. Preparation of Solution. The corrosion test was carried out at room temperature in air-saturated aqueous solution of 3.5 wt.% NaCl prepared by dissolving 17.5 grams of analytical grade NaCl dissolved in deionized water to make a 500 mL solution.

2.2. Methods

2.2.1. Potentiodynamic Polarization Method–Tafel Plot. Electrochemical measurements were carried out in a single compartment cell using a standard three-electrode setup: Ag/AgCl (3 M KCl) as a reference electrode, a platinum sheet

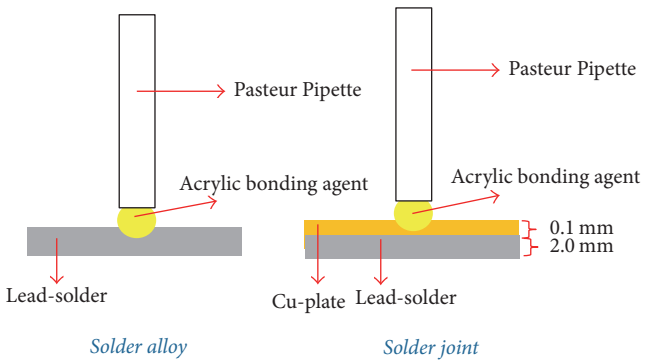

Figure 2: Preparation of samples for leaching measurements.

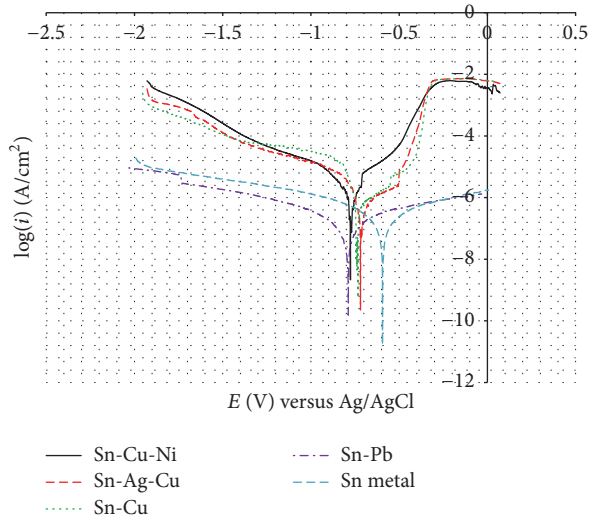

Figure 3: Potentiodynamic polarization curves of Sn and solder alloys in 3.5 wt.% NaCl solution under N_2 atmosphere. Scan range: from −1500 to 500 mV; scan rate: 1.00 mV/s; step potential: 0.45 mV.

(0.64 cm^2) as a counter electrode, and the lead-free solders as the working electrode. All the measurements were done under N_2 conditions. Metrohm Autolab PGSTAT 128 N was used as an electrochemical interface to control and record the potential. The samples were immersed in 250 mL corrosive medium inside the cell at room temperature for 180 s to attain a steady-state potential or open circuit potential (OCP). Potentiodynamic polarization curves were determined at −1500 to 500 mV range distinctive for the lead-free solder used on the study at an ASTM scan rate of 1.00 mV/s; step potential is at 0.45 mV and is presented in the form of typical polarization curves log I versus voltage. From the Tafel plot, the corrosion current (I_{CORR}), corrosion potential (E_{CORR}), polarization resistance (R_p), and corrosion rate (CR) of the metal alloys were calculated using the corrosion rate, Tafel slope method (Autolab application note COR02).

2.2.2. Leaching Measurements. For the leaching/dissolution measurement, the method by Cheng et al. [25] was adopted with slight modification. Small test cells containing 15 mL of test solutions were placed in a temperature-controlled oil bath at 45 ± 3°C. Every 3 days, oxygen was injected into the test solutions by gas flowmeter with a flow rate of 46 mL/min for 5 mins to keep the solution under low saturation of oxygen. Two mL of fresh test solutions was added to the test cell every 7 days or when the solution is reduced to keep the solution at 15 mL. The testing periods were done for 7, 15, and 30 days. After immersion for the subscribed period, 15 mL was taken and diluted into a 25 mL volumetric flask with deionized water. If there exists some precipitation in the test solution, sodium phosphate solution was used to dissolve the precipitates. The concentration of Sn in the diluted solution was analyzed using Atomic Absorption Spectrophotometer (Shimadzu AA-6300 Atomic Absorption Spectrophotometer) and the leaching amount per surface area of each element in the solders and their joints were calculated.

2.2.3. Surface Morphology and Elemental Analysis. The corroded surfaces of the samples were investigated using field-emission scanning electron microscopies (FESEM) (JEOL JSM-5310) and SEM (JEOL JSM-6500F) both equipped with an energy dispersive X-ray spectroscopy (EDS). X-ray diffraction (XRD) measurements were performed with a diffractometer (Rigaku Ultima IV) using Cu-Kα radiation (λ = 1.5405 Å) at an accelerating voltage of 40 kV. The diffracted beam was scanned in steps of 0.02° across a 2θ range of 20–90°.

3. Results and Discussion

3.1. Potentiodynamic Polarization Method–Tafel Plot. The Sn-0.7CuNi0.05 (referred to herein as Sn-Cu-Ni) in 3.5 wt.% NaCl solution showed a Tafel plot positioned at (E_{corr}) −0.78 mV versus Ag/AgCl (Figure 3). As compared to Sn-3.0Ag-05Cu (referred to herein as Sn-Ag-Cu) and Sn-0.8Cu (referred to herein as Sn-Cu) alloys, there is an observed shift of corrosion potential E_{corr} of lead-free solders to a less negative value following the sequence Sn-Cu-Ni < Sn-Cu < Sn-Ag-Cu. During the anodic polarization process, a stable passivation film is formed on the surface of the metal alloys *(vide infra)*. This passivation film determines the corrosion behaviour of the solder in the given media. The shift to a less negative potential signifies a formation of a more stable passivation film [26], which protects the solders and increases their corrosion resistance. The polarization resistance (R_p) data (Table 1) showed that Sn-Pb solder has the highest R_p (805.250 KΩ) and lowest corrosion rate (0.1949 $\times 10^{-2}$ mm/yr) compared to the lead-free solders. Between the three lead-free solder alloys, Sn-Cu-Ni showed the highest corrosion rate and Sn-Ag-Cu showed the lowest corrosion rate in 3.5 wt.% NaCl solution.

3.1.1. Microstructure Characterization of the Lead-Free Solders. The microstructure of solders before potentiodynamic polarization (Figure 4(a)) is a smooth surface showing the polishing lines and EDS analysis confirms the elemental

Table 1: Summary of corrosion parameters of metal alloys in 3.5 wt.% NaCl solution.

Sample	E_{corr} (V) versus Ag/AgCl	I_{corr} (μA/cm^2)	R_p (kΩ)	CR (mm/yr) $\times 10^{-2}$
Sn-Cu-Ni	−0.78	8.98	14.94	4.87
Sn-Ag-Cu	−0.73	3.06	43.86	1.71
Sn-Cu	−0.75	3.91	28.26	2.07
Sn-Pb	−0.79	0.39	805.25	0.19
Sn	−0.59	0.55	406.02	0.23

E_{corr}: corrosion potential, I_{corr}: corrosion current density, R_p: polarization resistance, and CR: corrosion rate.

Table 2: Surface element concentration of different solders before potentiodynamic polarization in 3.5 wt.% NaCl solution.

	Surface element composition (atom%)				
	Sn	Ag	Cu	Ni	Pb
Sn-Cu-Ni	98.59	-	1.27	0.14	-
Sn-Ag-Cu	96.74	2.74	0.52	-	-
Sn-Cu	98.97	-	1.38	-	-
Sn-Pb	59.03	-	-	-	40.97
Sn	100.00	-	-	-	-

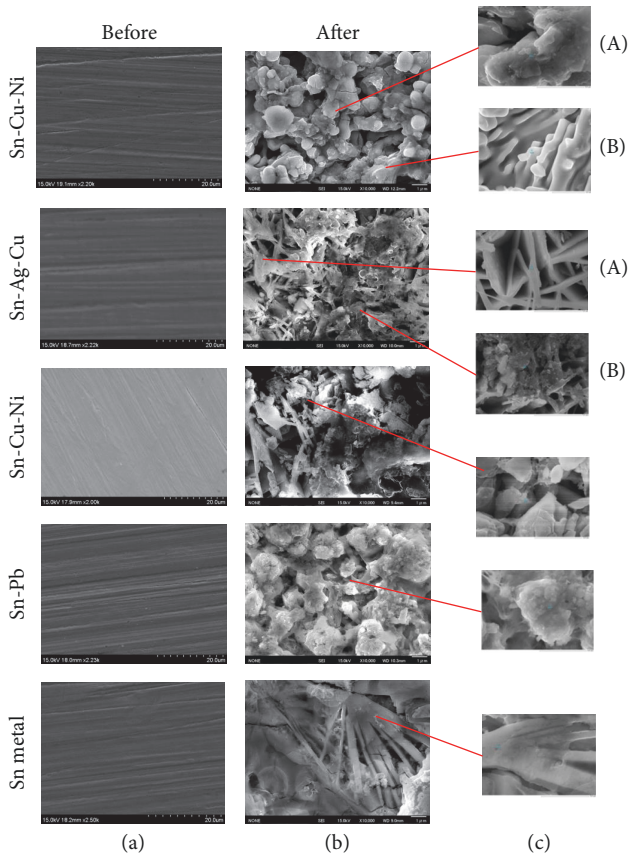

Figure 4: The microstructure of the metal surfaces on different solders before (a), after (b), and distinct morphologies on specified points (c) after potentiodynamic polarization tests in 3.5 wt.% NaCl solution.

composition of each solder (Table 2). After potentiodynamic polarization in 3.5 wt.% NaCl solution (Figure 4(b)), the microstructure of corroded Sn-Cu-Ni alloy had a porous flake-like surface while the Sn-Ag-Cu and Sn-Cu solders showed fibrous network oriented randomly on the surface in agreement with the observations of Li et al., [20]. Notable is the flake-like microstructures in Sn-Cu-Ni, which is similar in some respect to the Sn-Pb alloy. The EDS analysis on the surface of the corroded samples on each specified point was determined (Figure 4(c) and Table 3) and revealed the presence of Sn, O, and Cl indicating that the corrosion products are composed of the oxides and chlorides of tin. In conventional electrochemical reaction, Sn acts as an anode and reacts with Cl^- from the medium to form $SnCl_2$, which results in pitting and severed dissolution of Sn [27].

The cross-section of the metals after potentiodynamic polarization (Figure 5) showed visible corrosion layers distinct from the bulk metal. EDS analysis of the cross-section area (Table 4) for both lead and lead-free solders showed the top layer having similar corrosion products composed of Sn-rich and O-rich areas with <1% Cl. The Sn-Pb solder showed an outer layer rich in O while the inner layer was rich in Sn. The formation of oxides on the surface of the Sn-Pb solder indicates the presence of a stable passivation film that protects the metal from corroding. This explains why Sn-Pb solder has a better corrosion resistance than lead-free solders. In the case of the lead-free solders, since they have a different composition than Sn-Pb, the thin layer of oxides that formed on the surface of the alloy is not enough to protect the metal from the electrochemical process.

Table 3: Surface element concentration of different solders *after* potentiodynamic polarization in 3.5 wt.% NaCl solution on specific points as indicated in Figure 4(c).

	Surface element concentration (atom%)						
	Sn	Ag	Cu	Pb	Ni	Cl	O
Sn-Cu-Ni (A)	20.40	-	1.90	-	-	3.50	74.20
Sn-Cu-Ni (B)	56.70	-	0.80	-	-	0.20	42.30
Sn-Ag-Cu (A)	23.60	-	-	-	-	8.70	67.70
Sn-Ag-Cu (B)	32.30	-	0.20	-	-	12.10	55.40
Sn-Cu	20.50	-	0.10	-	-	10.70	68.70
Sn-Pb	28.40	-	-	-	-	0.60	71.00
Sn	29.90	-	-	-	-	15.00	55.10

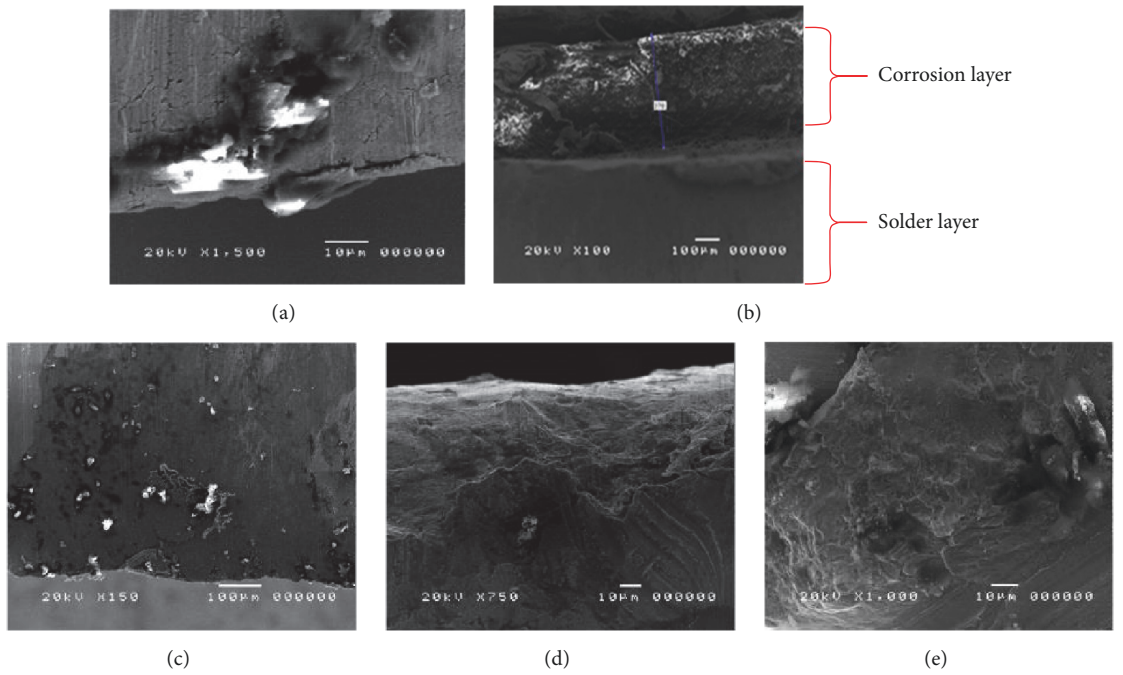

Figure 5: Cross-section image of the solders after potentiodynamic polarization test in 3.5 wt.% NaCl solution. (a) Sn; (b) Sn-Pb; (c) Sn-Ag-Cu; (d) Sn-Cu-Ni; (e) Sn-Cu.

3.1.2. Phase Composition Analysis of Corrosion Product on the Surface of the Solder Sample. The XRD diffractograms of corrosion products (Figure 6) showed corresponding XRD peaks attributed to tin oxides (SnO and SnO_2) and some chlorides. When compared with the XRD results of Yan and Xian [28] peaks for tin hydroxide ($Sn(OH_2)$) were also observed particularly for Sn-Pb and Sn metal [25]. These oxides effectively protect the metal. The oxides, however, were not visibly detected in Pb-free solders indicating nil or minimal formation of the passivation layer.

During potentiodynamic polarization measurements, the reduction of oxygen in the neutral aqueous solution (1) initially occurs [20]

$$4e^- + O_2 + 2H_2O \longrightarrow 4OH^-. \quad (1)$$

Once the current reaches 10 mA/cm^2, bubbles were observed from the solution caused by the evolution of hydrogen from the cathode.

$$2H_2O + 2e^- \longrightarrow H_2 + 2OH^-. \quad (2)$$

The following plausible anodic reactions would occur [17, 19]:

$$Sn \longrightarrow Sn^{2+} + 2e^- \quad (3)$$

$$Sn^{2+} \longrightarrow Sn^{4+} + 2e^- \quad (4)$$

$$Sn + 2OH^- - 2e^- \longrightarrow Sn(OH)_2 \quad (5)$$

$$Sn + 2OH^- - 2e^- \longrightarrow SnO + H_2O \quad (6)$$

$$2Sn + O_2 + 6H_2O \longrightarrow 2Sn(OH)_2 \quad (7)$$

$$Sn(OH)_2 + 2OH^- - 2e^- \longrightarrow Sn(OH)_4 \quad (8)$$

$$2Sn^{2+} + 6H_2O + O_2 \longrightarrow 2Sn(OH)_4 + 4H^+. \quad (9)$$

Formation of tin oxides is thermodynamically favourable thus tin hydroxides can dehydrate easily to form SnO and SnO_2 [25, 29]. Although not detected in XRD due to its trace concentration relative to Sn, the potential corrosion products

Table 4: Cross-section element concentration of different solders after Potentiodynamic polarization tests in 3.5 wt.% NaCl solution.

	Cross-section element concentration (atom%)						
	Sn	Ag	Cu	Ni	Pb	Cl	O
Sn-Cu-Ni							
Top layer	63.99	-	0.60	0.22	-	0.92	33.91
Inner layer	98.59	-	1.27	0.14	-	-	-
Sn-Ag-Cu							
Top layer	40.95	1.12	0.17	-	-	0.15	57.27
Inner layer	97.36	2.01	0.63	-	-	-	-
Sn-Cu							
Top layer	64.58	-	0.72	-	-	0.60	33.35
Inner layer	99.30	-	0.70	-	-	-	-
Sn-Pb							
Top layer	6.85	-	-	-	3.91	0.91	88.03
Inner layer	60.16	-	-	-	39.84	-	-
Sn							
Top layer	32.62	-	-	-	-	0.37	66.41
Inner layer	99.85	-	-	-	-	0.15	-

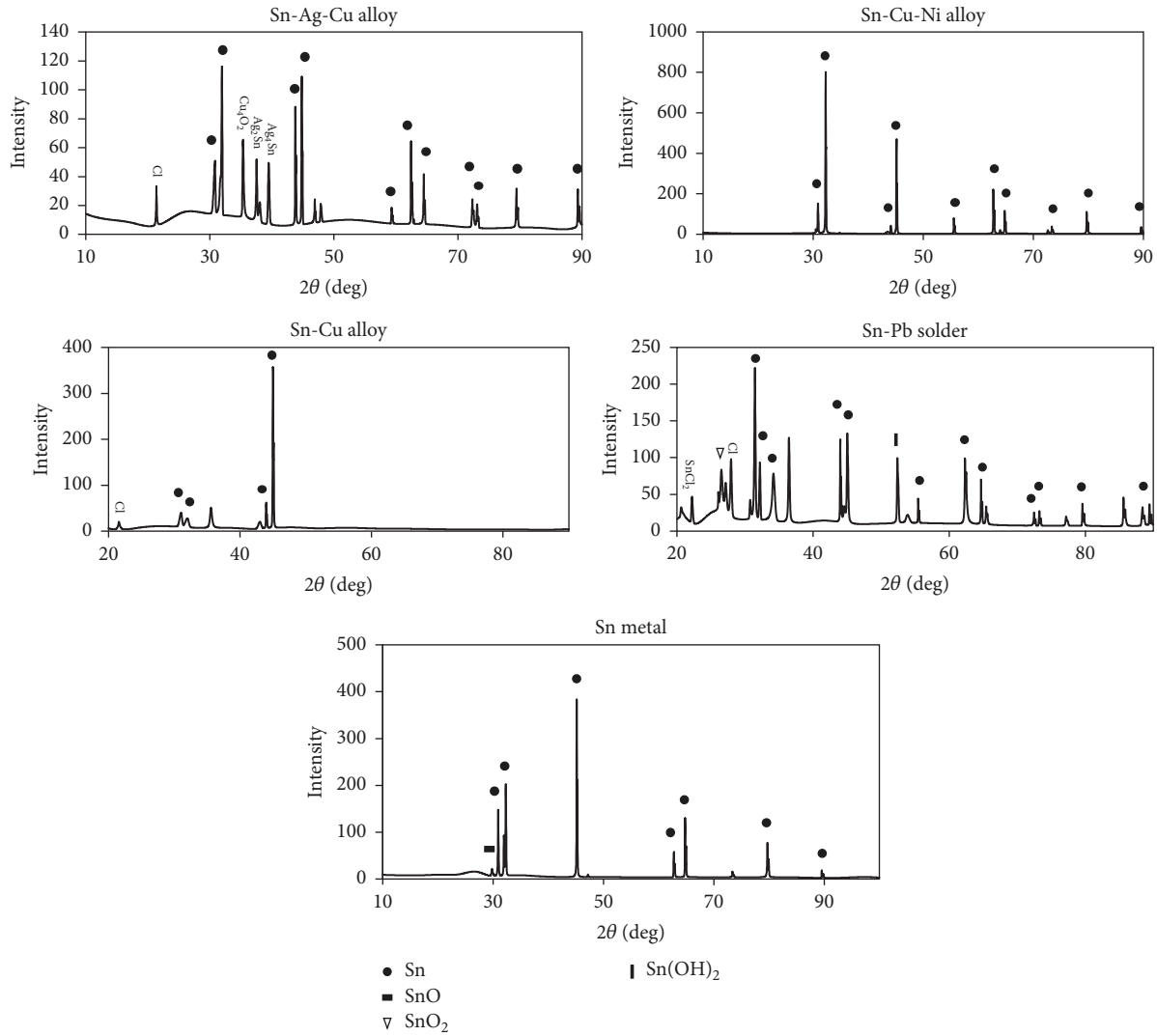

Figure 6: XRD patterns of surface product on different solder material after potentiodynamic polarization test.

of copper and nickel are metal chlorides. Corrosion of copper is dependent on the presence of chloride ions either through direct formation of cupric chloride

$$\mathrm{Cu} \longleftrightarrow \mathrm{Cu}^{+} + \mathrm{e}^{-} \quad (10)$$

$$\mathrm{Cu}^{+} + 2\mathrm{Cl}^{-} \longleftrightarrow \mathrm{CuCl}_2{}^{-} \quad (11)$$

or through the electro-dissolution of copper [30]

$$\mathrm{Cu} + \mathrm{Cl}^{-} \longleftrightarrow \mathrm{CuCl} + \mathrm{e}^{-} \quad (12)$$

$$\mathrm{CuCl} + \mathrm{Cl}^{-} \longleftrightarrow \mathrm{CuCl}_2{}^{-}. \quad (13)$$

The anodic polarization of copper alloys in NaCl solution lowers the fracture stresses as measured in slow strain experiments making copper alloys under cyclic stresses to have lower service lives in chloride solutions [31]. Thus, chlorides penetrate into the material crevices allowing for corrosion of susceptible atoms such as copper to occur. For nickel corrosion, the initial step is nickel hydration to facilitate dissolution and this can occur when water transport into the material is enhanced. The transport of water is dependent on chloride environment. This was observed when we compared the potentiodynamic polarization of Sn-Cu-Ni alloy in neutral chloride-containing medium ($E_{corr} = -0.776$ V versus Ag/AgCl, $I_{corr} = 8.982\,\mu A/cm^2$) and in acidic chloride-free electrolyte (0.1 M HNO_3; $E_{corr} = -0.356$ V versus Ag/AgCl, $I_{corr} = 4.34\,\mu A/cm^2$). A sudden shift of corrosion potential to a less negative value is observed attributed to the formation of the passivation film. The absence of chloride in HNO_3 medium promotes barrier creation preventing hydration and corrosion to occur. This suggests that Sn-Cu-Ni alloy has high corrosion resistance in an acidic chloride-free environment. Chlorides even in small amounts can break the protective films initiating the occurrence of corrosion.

3.2. Soldering Properties and Leaching Measurements. During the preparation of the solder joints with copper substrates, a better surface finish of the joints was observed when Sn-Cu-Ni solder was used compared to Sn-Cu alloys. The design of adding Ni to common Sn-Cu alloy improved the soldering property [32]. These observations were consistent with the unique morphology of the intermetallic compound (IMC) layer reported by Harcuba et al. [33]. The IMC was described as noncompact islands of solder entrapped in the IMC phase and that the IMC layer contains more Ni than the solder. Nickel addition promoted the significant acceleration of the growth kinetics of the IMC layer.

The solder joints and the raw Pb-free solder alloys were subjected to corrosive media immersion to determine the leaching behaviour (Figure 7). The amount of Sn leached correlates with the corrosion rate of the alloys [25, 29, 34]. Since the results of potentiodynamic polarization test showed that all of the three Pb-free solders had higher corrosion rate than the Sn-Pb solder and Sn metal, leaching amounts of Sn were done only for the Pb-free solders. The leaching amounts of Sn after immersion in 3.5 wt.% NaCl solution after 30 days are observed to be greater for solder joints compared to its corresponding alloy. Sn-Ag-Cu alloy had the highest leaching

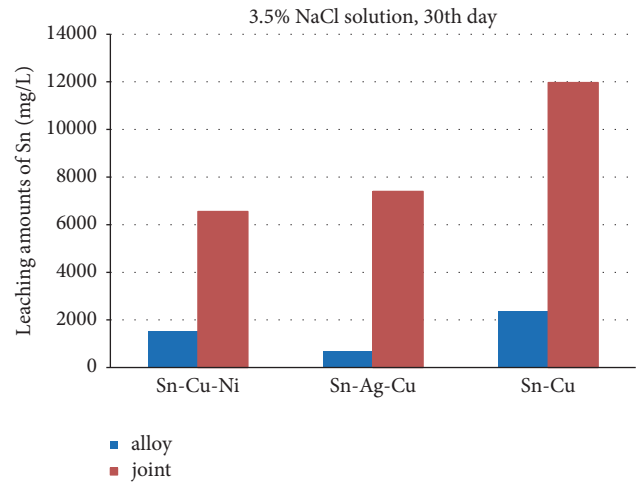

Figure 7: Atomic Absorption Spectroscopy (AAS) results on Tin (Sn) leaching from lead-free solder alloy and joint after 30 days.

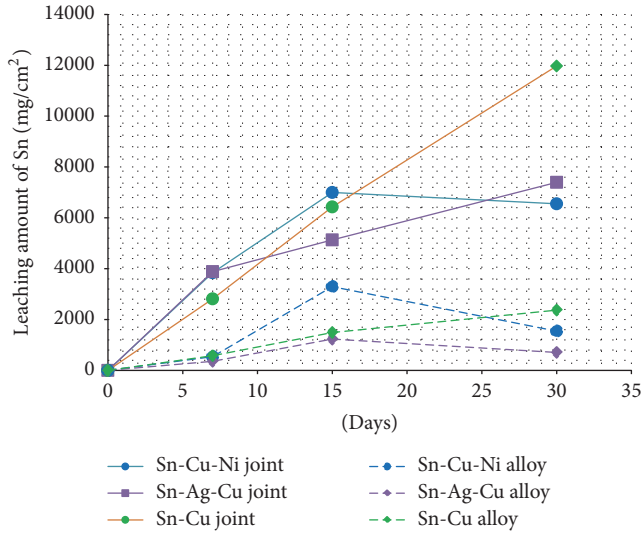

Figure 8: Leaching kinetics of Sn from Sn-Ag-Cu, Sn-Cu-Ni, and Sn-Cu alloy and their joints in 3.5 wt.% NaCl solution.

of Sn for the solder alloys followed by Sn-Cu alloy while Sn-Cu-Ni had the lowest leaching amount after 30 days. For solder joints, leached Sn follows the order Sn-Cu > Sn-Ag-Cu > Sn-Cu-Ni.

Leaching kinetics of Sn from the metals (Figure 8) show that solder joints gave a higher amount of leached Sn compared to their alloy counterparts. The use of Cu-substrate in the solder joint setup affects the leaching behaviour of Sn. This is because dissimilar metals having different oxidation potentials in contact with each other experience galvanic corrosion [25, 29], which does not occur in solder alloys alone. According to Lao et al., [29] the current density of the solder joint is almost twofold higher than its corresponding solder alloy. Thus, the galvanic cell (anode = Sn; cathode = Cu) accelerates the leaching amount of Sn from the joint.

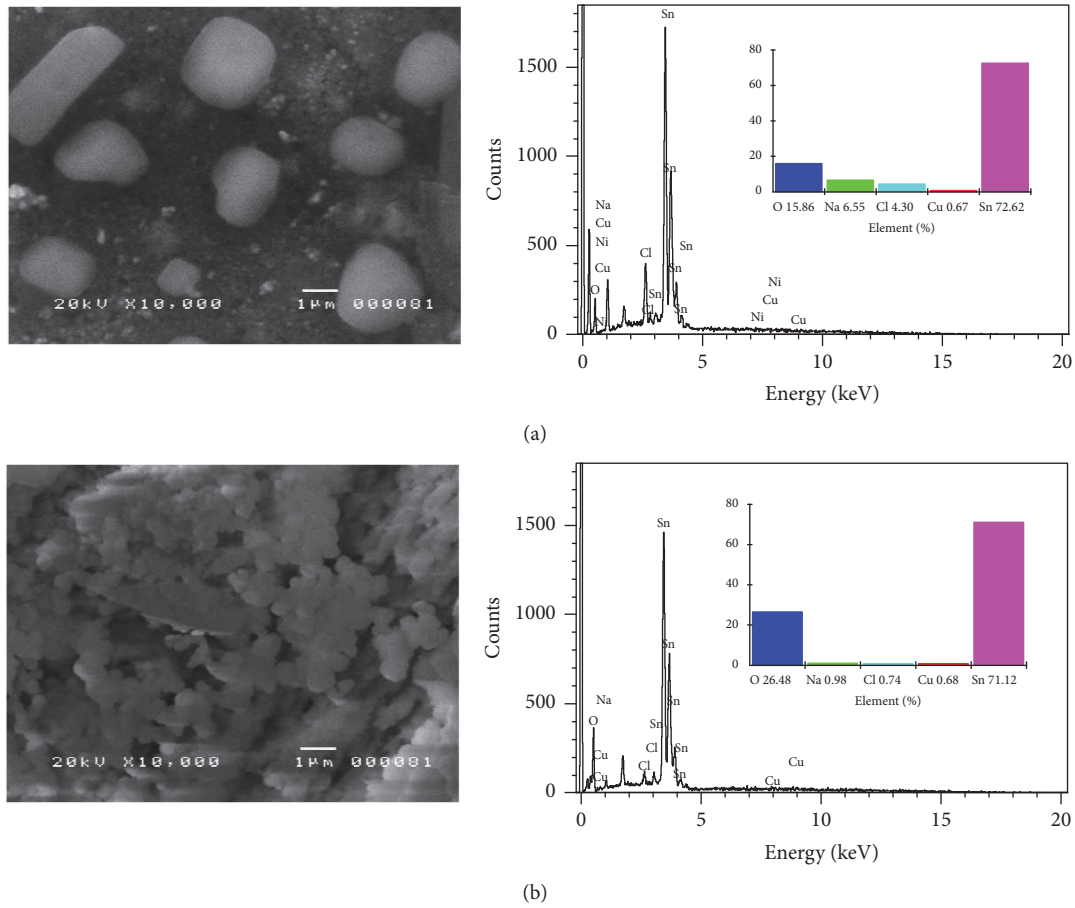

Figure 9: Surface morphology analysis of Sn-Cu-Ni (a) solder alloy and (b) solder joint and their corresponding EDS spectra after 30-day leaching measurements in 3.5 wt.% NaCl solution.

The microstructure analysis of Sn-Ni-Cu solder after 30-day immersion in NaCl solution (Figure 9) showed a more corroded surface for the joint and microstructure is composed of platelet-like materials on the surface. EDS analysis on the surface showed high amounts of Sn and O suggesting that the corrosion products are composed primarily of oxides of Sn and small amounts of chlorides. This is further confirmed by the detection of XRD patterns specific to SnO_2 (Figure 10). Similarly, corresponding peaks for $Sn(OH)_2$ were detected from Yan and Xian [28].

3.2.1. Microstructure of Corrosion Products on Solder Surface. The microstructures of the corrosion surface were monitored as the exposure to the corrosive media increases. Generally, as the alloy (Figure 11) was exposed to the salt solution, the surface changed dramatically from smooth to porous with the formation of plate-like structures attributed to the weakly bonded corrosion products that form on the surface. These compounds, which have been identified in EDS and XRD as oxides of tin are typical corrosion products. The formation of these compounds is a result of a charge transfer reaction between Sn metal, salt ion, atmospheric O_2, and H_2O during anodic polarization following the mechanism proposed by Mohran et al. [35]. These corrosion products are weakly held by the bulk metal and can easily chip-off into the solution in agreement with the leaching experiments. The microstructural changes that can be observed for Sn-Cu-Ni are the noticeable degree of high corrosion product (platelet-like structure) after 7-day exposure compared to Sn-Ag-Cu and Sn-Cu. The corrosion products are formed along the cracks, which allow the water to seep-in triggering the corrosion reaction. As the exposure time increases, the entire surface was covered with corrosion products.

For the solder joints, the microstructure changes were likewise monitored (Figure 12). A more dramatic morphology can be observed characterized by branched crystallites, sponge-like structure, networked branches, and platelet-like materials. The formation of these microstructures occurs within 7-day exposure and increases gradually as time increases. This is the consequence of galvanic reaction that occurs since the solder joints are in contact with the Cu metal as substrate. The galvanic reaction triggers the very fast corrosion process. The EDS analysis of these microstructures reveals O and Sn-rich surface indicating oxides of Sn formation, which was further confirmed by XRD as SnO_2 (Figure 10).

Generally, the surfaces of the alloys show some corrosion product as evidenced by the plate-like structures. The surfaces

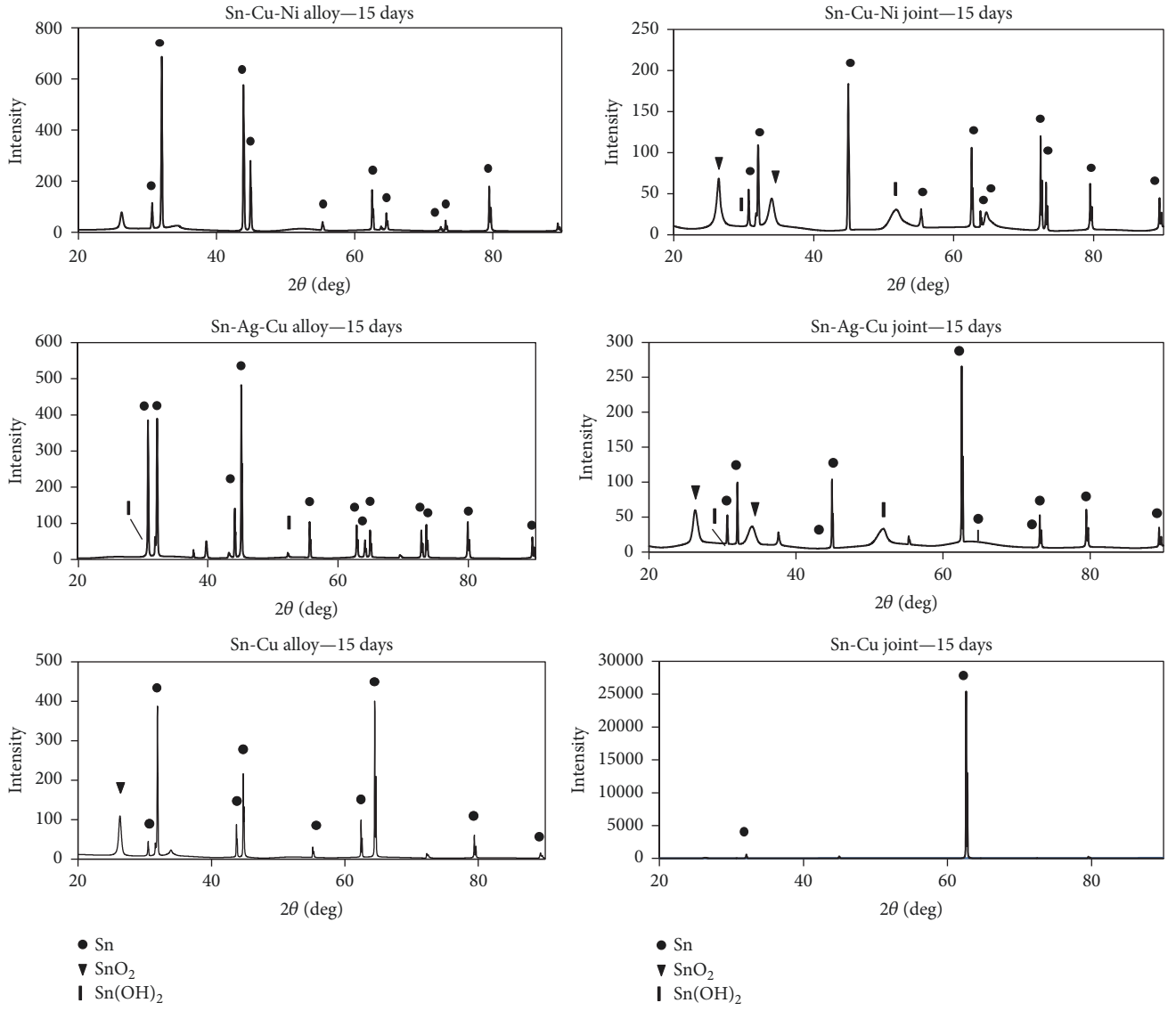

Figure 10: XRD patterns of surface product of Sn-Ag-Cu, Sn-Cu-Ni, and Sn-Cu solder alloy and joint after 15-day immersion in 3.5 wt.% NaCl solution.

are covered by a small degree of corrosion layer suggesting minimal corrosion on the alloy surface. However, the surface of the joint showed a high degree of corrosion with the entire surface covered with corrosion products forming nanocrystals and sponges. Similar morphology was reported by Lao et al., [29] in the leaching measurement of Sn-0.75Cu solder alloy and joint in simulated soil solutions. The corrosion layer formed on the surface of the alloy forms a protecting film that has a shielding effect on the Sn ion transport between the solder and the solution. However, in the case of the solder joint, the loosely bound corrosion layer can break-off easily. The corrosion products that made up the surface would no longer protect the substrate resulting in plenty of leaching amounts of Sn coming from the solder joint.

The result of potentiodynamic polarization and leaching tests in 3.5 wt.% NaCl solution is conflicting. Results for the Tafel extrapolation show that Sn-Cu-Ni has the highest corrosion rate, while the 30-day immersion of the solder alloy and joint in NaCl solution showed the lowest amount of leached Sn for all the solders understudied. This was attributed to the rapid analysis in an electrochemical process, where corrosion is forcedly induced on the surface of the metal by applying voltage. A rapid measurement can influence the formation of the passivation film on the surface of the metal. On the other hand, the long exposure time with the corrosive media in leaching experiments allows an actual electrochemical process to occur and measured progressively. In these conditions, the formation of corrosion product is gradual and there is longer timeframe for the stabilization and formation of the passivation film.

These results are significant since, in electronic processes, the solder alloy is not used alone. Rather it is used in contact with other metals mostly Cu in most electronic substrates. These lead-free solders therefore, once in a corrosive media

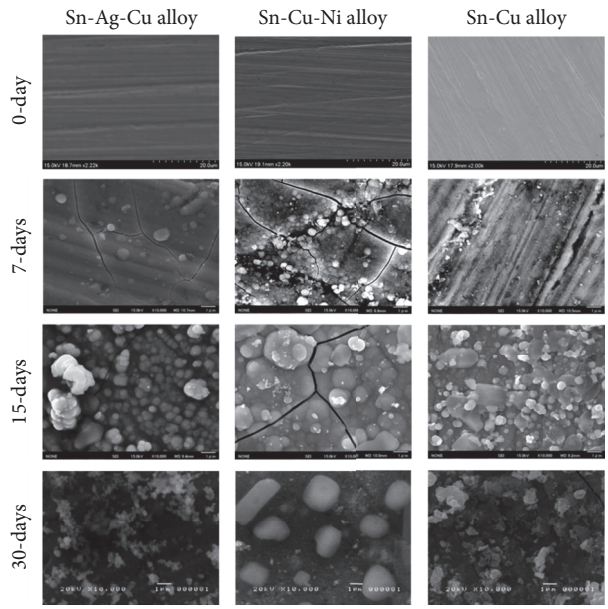

Figure 11: SEM image of lead-free solder alloy after 7, 15, and 30 days leaching measurement in 3.5 wt.% NaCl solution.

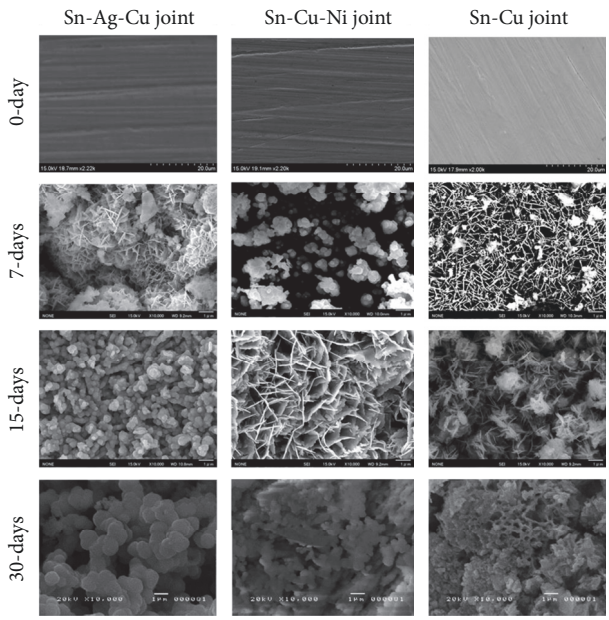

Figure 12: SEM image of lead-free solder joint after 7, 15, and 30 days leaching measurement in 3.5 wt.% NaCl solution.

such as aqueous NaCl atmosphere, are prone to corrosion even within 7 days of exposure. The corrosion reaction is triggered by the galvanic reaction that occurs when this happens inside an electronic gadget. The interconnections and electrical connectivity are lost affecting the form, features, and function of the device.

4. Conclusions

The corrosion behaviour of Sn-Cu-Ni lead-free solder was described for the first time. In 3.5 wt.% NaCl environment, potentiodynamic polarization test revealed that the new Sn-Cu-Ni solder has higher corrosion rate compared to Sn-Cu and Sn-Ag-Cu. However, longer exposure of the Sn-Cu-Ni alloy and joint to the corrosive medium for up to 30 days showed the lowest leaching rate of Sn compared to Sn-Cu and Sn-Ag-Cu solders. Generally, alloys have lower leaching rate compared to the corresponding joint due to the galvanic reaction occurring in the joint setup. For chloride-containing solution, the corrosion and leaching behaviour of Sn-Ag-Cu is better compared to Sn-Ni-Cu and Sn-Cu. Further study is underway in acidic and basic media and will be reported elsewhere.

Conflicts of Interest

There are no conflicts of interest related to this paper.

Acknowledgments

This work was supported by the Accelerated Science and Technology Human Resource Development Program (ASTHRDP) of the Department of Science and Technology, Science Education Institute (DOST-SEI). Jan-Ervin C. Guerrero is grateful for the Japan Sakura Science Program.

References

[1] M. Abtew and G. Selvaduray, "Lead-free solders in microelectronics," *Materials Science and Engineering: A Structural Materials: Properties, Microstructure and Processing*, vol. 27, no. 5, pp. 95–141, 2000.

[2] S. Tong, Y. von Schirnding, and T. Prapamontol, "Environmental lead exposure: a public health problem of global dimensions," *Bulletin of the World Health Organization*, 2000, http://www.who.int/bulletin/archives/78(9)1068.pdf.

[3] J. H. Lau and K. Liu, "Global Trends in Lead-free soldering," *International Journal of Advanced Packaging Technology*, vol. 13, no. 2, pp. 25–28, 2004.

[4] S. Garesan and M. Pecht, *Lead Free Electronics*, IEEE Press/John Wiley & Sons. Inc, Hoboken, NJ, USA, 2006.

[5] K. Suganuma, "Advances in lead-free electronics soldering," *Current Opinion in Solid State & Materials Science*, vol. 5, no. 1, pp. 55–64, 2001.

[6] N. Chawla, "Thermomechanical behaviour of environmentally benign Pb-free solders," *International Materials Reviews*, vol. 54, no. 6, pp. 368–384, 2009.

[7] K. Zeng and K. N. Tu, "Six cases of reliability study of Pb-free solder joints in electronic packaging technology," *Materials Science and Engineering: Reports*, vol. 38, no. 2, pp. 55–106, 2002.

[8] D. K. Mu, S. D. McDonald, J. Read, H. Huang, and K. Nogita, "Critical properties of Cu6Sn5 in electronic devices: recent progress and a review," *Current Opinion in Solid State & Materials Science*, vol. 20, no. 2, pp. 55–76, 2016.

[9] H. R. Kotadia, P. D. Howes, and S. H. Mannan, "A review: on the development of low melting temperature Pb-free solders," *Microelectronics Reliability*, vol. 54, no. 6-7, pp. 1253–1273, 2014.

[10] G. Zeng, S. McDonald, and K. Nogita, "Development of high-temperature solders: review," *Microelectronics Reliability*, vol. 52, no. 7, pp. 1306–1322, 2012.

[11] H. Nishikawa, J. Y. Piao, and T. Takemoto, "Effect of Ni addition on interfacial reaction between Sn-Cu solder and Cu base metal," in *Joining of Advanced and Specialty Materials VII, Proceedings from Materials Solutions 2004 on Joining of Advanced and Specialty Materials*, T. J. Lienert, Ed., vol. 35, pp. 208–211, Columbus, OH, USA, October 2006.

[12] B. L. Silva, N. Cheung, A. Garcia, and J. E. Spinelli, "Evaluation of solder/substrate thermal conductance and wetting angle of Sn–0.7 wt%Cu–(0–0.1 wt%Ni) solder alloys," *Materials Letters*, vol. 142, pp. 163–167, 2015.

[13] J.-W. Yoon, B.-I. Noh, B.-K. Kim, C.-C. Shur, and S.-B. Jung, "Wettability and interfacial reactions of Sn-Ag-Cu/Cu and Sn-Ag-Ni/Cu solder joints," *Journal of Alloys and Compounds*, vol. 486, no. 1-2, pp. 142–147, 2009.

[14] L. Yang, J. Ge, Y. Zhang, J. Dai, H. Liu, and J. Xiang, "Investigation on the Microstructure, Interfacial IMC Layer, and Mechanical Properties of Cu/Sn-0.7Cu-xNi/Cu Solder Joints," *Journal of Electronic Materials*, vol. 45, no. 7, pp. 3766–3775, 2016.

[15] H. Nishikawa, J. Y. Piao, and T. Takemoto, "Interfacial reaction between Sn-0.7Cu (-Ni) solder and Cu substrate," *Journal of Electronic Materials*, vol. 35, no. 5, pp. 1127–1132, 2006.

[16] S. Farina and C. Morando, "Comparative corrosion behaviour of different Sn-based solder alloys," *Journal of Materials Science: Materials in Electronics*, vol. 26, no. 1, pp. 464–471, 2014.

[17] K. Pietrzak, M. Grobelny, K. Makowska et al., "Structural aspects of the behavior of lead-free solder in the corrosive solution," *Journal of Materials Engineering and Performance*, vol. 21, no. 5, pp. 648–654, 2012.

[18] M. Reid and L. F. Garfias-Mesias, "Corrosion of electronics: lead-free initiatives," in *Uhlig's Corrosion Handbook*, R. W. Revie, Ed., pp. 565–570, John Wiley & Sons, Inc, Hoboken, NJ, USA, 3rd edition, 2011.

[19] K.-L. Lin and T.-P. Liu, "The electrochemical corrosion behaviour of Pb-free Al-Zn-Sn solders in NaCl solution," *Materials Chemistry and Physics*, vol. 56, no. 2, pp. 171–176, 1998.

[20] D. Li, P. P. Conway, and C. Liu, "Corrosion characterization of tin-lead and lead free solders in 3.5 wt.% NaCl solution," *Corrosion Science*, vol. 50, no. 4, pp. 995–1004, 2008.

[21] W. R. Osório, E. S. Freitas, J. E. Spinelli, and A. Garcia, "Electrochemical behavior of a lead-free Sn-Cu solder alloy in NaCl solution," *Corrosion Science*, vol. 80, pp. 71–81, 2014.

[22] M. Liu, W. Yang, Y. Ma, C. Tang, H. Tang, and Y. Zhan, "The electrochemical corrosion behavior of Pb-free Sn-8.5Zn-XCr solders in 3.5 wt.% NaCl solution," *Materials Chemistry and Physics*, vol. 168, pp. 27–34, 2015.

[23] A. Kamarul Asri and E. Hamzah, "Corrosion behaviour of lead-free and Sn-Pb solders in 3.5wt% NaCl," *Advanced Materials Research*, vol. 686, pp. 250–260, 2013.

[24] U. S. Mohanty and K.-L. Lin, "Electrochemical corrosion behaviour of Pb-free Sn-8.5Zn-0.05Al-XGa and Sn-3Ag-0.5Cu alloys in chloride containing aqueous solution," *Corrosion Science*, vol. 50, no. 9, pp. 2437–2443, 2008.

[25] C. Q. Cheng, F. Yang, J. Zhao, L. H. Wang, and X. G. Li, "Leaching of heavy metal elements in solder alloys," *Corrosion Science*, vol. 53, no. 5, pp. 1738–1747, 2011.

[26] A. Wierzbicka-Miernik, J. Guspiel, and L. Zabdyr, "Corrosion behavior of lead-free SAC-type solder alloys in liquid media," *Archives of Civil and Mechanical Engineering*, vol. 15, no. 1, pp. 206–213, 2015.

[27] A. Sharma, S. Das, and K. Das, "Electrochemical corrosion behavior of CeO_2 nanoparticle reinforced Sn-Ag based lead free nanocomposite solders in 3.5wt.% NaCl bath," *Surface and Coatings Technology*, vol. 261, pp. 235–243, 2015.

[28] Z. Yan and A.-P. Xian, "Corrosion of Ga-doped Sn-0.7Cu solder in simulated marine atmosphere," *Metallurgical and Materials Transactions A: Physical Metallurgy and Materials Science*, vol. 44, no. 3, pp. 1462–1474, 2013.

[29] X.-D. Lao, C.-Q. Cheng, X.-H. Min et al., "Corrosion and leaching behaviors of Sn-based alloy in simulated soil solutions," *Transactions of Nonferrous Metals Society of China*, vol. 26, no. 2, pp. 581–588, 2016.

[30] F. Arjmand and A. Adriaens, "Influence of pH and chloride concentration on the corrosion behavior of unalloyed copper in NaCl solution: a comparative study between the micro and macro scales," *Materials*, vol. 5, no. 12, pp. 2439–2464, 2012.

[31] B. D. Craig and D. S. Anderson, Eds., *Handbook of Corrosion Data*, ASM International, Materials Park, OH, USA, 2nd edition, 1995.

[32] T. Ventura, C. M. Gourlay, K. Nogita, T. Nishimura, M. Rappaz, and A. K. Dahle, "The influence of 0-0.1 wt.% Ni on the microstructure and fluidity length of Sn-0.7Cu-xNi," *Journal of Electronic Materials*, vol. 37, no. 1, pp. 32–39, 2008.

[33] P. Harcuba, M. Janeček, and M. Slámová, "The effect of Cu and Ni on the structure and properties of the IMC formed by the reaction of liquid Sn-Cu based solders with Cu substrate," in *Proceedings of Contributed Papers (WDS '08)*, part III, pp. 220–224, Prague, Czech, June 2008.

[34] M. Mori, K. Miura, T. Sasaki, and T. Ohtsuka, "Corrosion of tin alloys in sulfuric and nitric acids," *Corrosion Science*, vol. 44, no. 4, pp. 887–898, 2002.

[35] H. S. Mohran, A.-R. El-Sayed, and H. M. Abd El-Lateef, "Anodic behavior of tin, indium, and tin-indium alloys in oxalic acid solution," *Journal of Solid State Electrochemistry*, vol. 13, no. 8, pp. 1279–1290, 2009.